

## 5 Flows with floating particles

In this chapter we present the main contribution of this thesis, a fictitious domain based formulation to perform numerical simulations of flows with particles suspended in two liquid phases that may also float at the interface between the phases. Our floating particles formulation is in fact an extension of the new approach described on the previous chapter that includes the horizontal and vertical components of the capillarity force action on all particles positioned over the fluids' interface. The present work fills a gap since there are no other methods available that describe the full dynamics of fluid-particle interactions, from the particles' fluidization until the action of the capillary force on particles floating at the fluid's surface.

This chapter is organized as follows: in the first section 5.1 we review previous works on numerical simulation of floating particles, section 5.2 presents our new formulation to simulate flow with suspended particles that may float.

### 5.1 Numerical simulation of floating particles

To the best of our knowledge, previous works on floating particles' simulation may be divided in two classes. The first class of floating particles methods (38) aims to develop numerical simulations for particle motions in fluid interfaces assuming that the particles are initially at rest over the interface. The particles move in a direct simulation satisfying the fundamental equations of motion of fluids and solid particles. The work of Singh et al (2005) (38) uses a Level Set method together with the fictitious domain method to simulate the equilibrium position of particles at the interface of two fluids and also to approximate the interface's geometry until the flow reaches its steady configuration.

The second class of works follows the approach used by Fujita et al (2006) (15) to develop structure formation simulators for colloidal particles during drying. In those works, instead of performing the full discretization of the Navier–Stokes equations and compute the interaction forces between the particles and the fluids explicitly, it describes the motion of the particles using models like the Langevin equations, in which forces exerted on each particle consist of contact, capillarity, Brownian, van der Waals, electrostatic and fluid drag forces.

Our work differs from the previous methods since it solves the fluid and rigid body fundamental equations to simulate particles that flow and float within the same simulation framework. In this way, with our method, we can perform studies to determine the final organization of a set of particles at the interface of two fluid phases, given random initial particles' positions inside the fluid's domain. As the second class of previous works, our approach can be used to develop structure formation simulators, but as in the first set of works, it uses a direct approach based on the fictitious domain technique. Moreover, in our approach, the capillarity forces are computed as an additional body force that acts on particles that are over the fluid phase's interface, which avoids the need for computing the interfacial deformation.

## 5.2

### Floating particles using fictitious domain

Our formulation to perform simulations of flows with suspended particles that can float is an extension of the one proposed in the previous chapter for flows with suspended particles. On the new problem, the fluid region is filled by two different fluid phases. By convention in a two–phase flow, we call the fluid phase with higher density by *water* and the lower density fluid by *air*, even when the physical properties of the fluid phases are different from the air and water properties.

To derive the new formulation, we need to include the effect of the capillarity forces, described in 2-7 and 2-8, in the final differential formulation of the equation that describes the particle's velocity 4-9, since in our approach, the capillarity force is treated as a body force acting on the particles that are on the interface between the fluid phases. Just to remember, we denote the capillarity force acting on the particle  $p_i$  by  $\vec{c}_{p_i}$  and now we adopt the following notation:

$$\vec{C}_{p_i} = \begin{cases} \vec{c}_{p_i} & \text{if } p_i \text{ intersects } \partial\Omega_{f_{ij}} \\ 0 & \text{otherwise} \end{cases} \quad (5-1)$$

As we can see from equation 5-1, the action of the capillarity force is restricted to particles that intersect the interface  $\partial\Omega_{f_i f_j}$  between two fluid phases  $f_i$  and  $f_j$  and as we see on the equations 2-7 and 2-8, it is written as a function of the immersed height of the particle. Recalling the capillarity force equations:

$$\vec{c}_{p_i}^h = 2\zeta \cos(\arccos(\frac{b_{p_i}}{R_{p_i}}) - \psi) \quad \text{and} \quad \vec{c}_{p_i}^v = 2\zeta \sin(\arccos(\frac{b_{p_i}}{R_{p_i}}) - \psi)$$

The variation of the absolute value of the components of the capillarity force given the immersed height measurement  $b_{p_i}$  is shown in Figure 5.1.

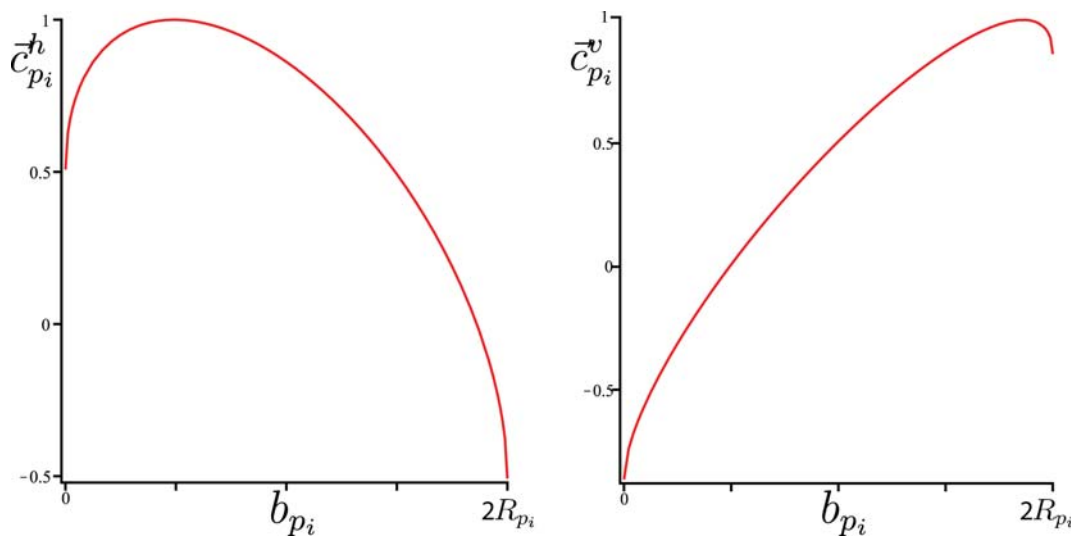


Figure 5.1: Graph of the capillarity force components in function of the immersed height. The picture on left shows the vertical component of the capillarity while the image on right shows its horizontal component.

It is important to observe that as we are not simulating the fluids' interface deformation, the computation of the immersed portion of a particle on the water phase is done by using the straight line that represents the static interface. This approximation introduces an error on the capillarity force computation, as shown in Figure 5.2. The region in red on the left image represents the area of the particle neglected by our capillarity force approximation. The error induced by this approximation is shown on the graphs on right. The curve in red represents the exact values of the force, while the gray curves represents the force obtained assuming an error of 5% on the height measurement.

Moreover, the horizontal component of the capillarity force is an interaction force between particles or between one particle and one of the domain's wall. In this way, it only acts when more than one particle floats together on the fluid phases' interface or when a particle is near the domain's wall. Its action must exponentially decrease as the distance between the particles increases,

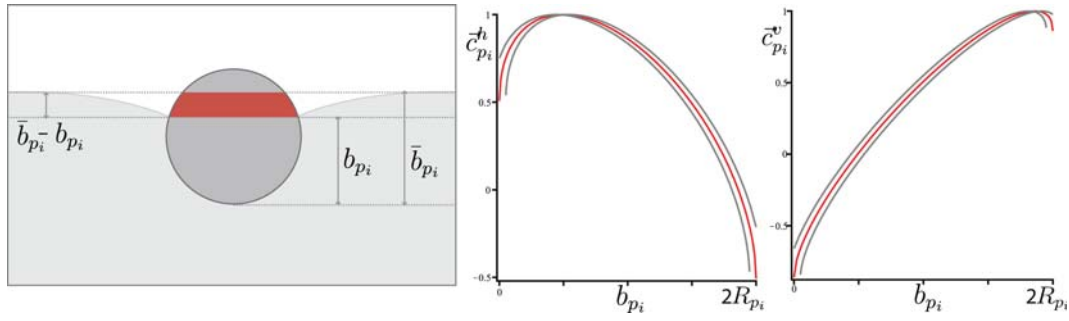


Figure 5.2: Error on the immersed height of the particles at the fluid phases' interface. The neglected area (left) and the effect on the capillarity force's absolute value (right)

so particles that are distant do not interact with each other. The expression for the horizontal component of the capillarity force is weighted by the following piecewise polynomial function that approximates a decreasing exponential function:

$$W(d) = \begin{cases} \frac{d^2}{4} - d + 1.0 & \text{if } 0 \leq d \leq 2 \\ 0 & \text{otherwise} \end{cases} \quad (5-2)$$

where  $d = \frac{2d_{ij}}{\delta R_{p_i}}$  and  $\delta \geq 1$  is the influence factor for the action of the capillarity force and  $d_{ij} = \|\vec{X}_{p_i} - \vec{X}_{p_j}\| - R_{p_i} - R_{p_j}$  is the distance between the center of the particles  $p_i$  and  $p_j$ . Figure 5.3 sketches the parameters used in the computation of the weighting function  $W$  (left image), and shows its behavior as we increases the distance between the two particles (right image).

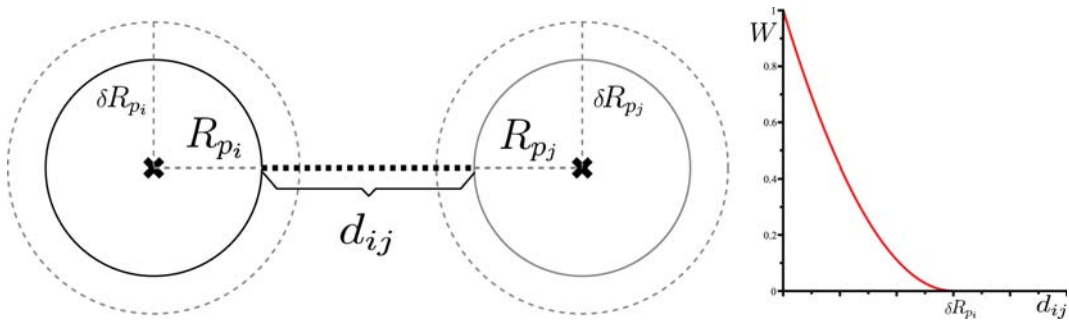


Figure 5.3: Sketch of the interaction between two particles that are floating on the fluid's surface at the left image, and the graph of the capillarity force's horizontal component in function of the distance between the particles.

We can now write the new version of the particle's velocity equation as:

$$\int_{\Omega_{p_i}} (\rho_{p_i} - \rho_f) \frac{\partial \vec{U}_{p_i}}{\partial t} d\Omega_{p_i} = \int_{\Omega_{p_i}} \rho_{p_i} \vec{g} - \nabla p + \vec{F} d\Omega_{p_i} + \vec{C}_{p_i} \quad (5-3)$$

We also include a repulsion force on the particle velocity equation to avoid interpenetration between particles. The repulsion force is computed using the same approach described by Glowinski et al (19).

Substituting the particle velocity equation from the previous particulate flow differential formulation and using the expression of the additional body force  $\vec{F}$  in terms of the Lagrange multipliers  $\vec{l}$ , we get the final formulation, used to compute the velocity  $\vec{u}$ , pressure  $p$ , Lagrange multipliers  $\vec{l}$  fields, the particle's linear and angular velocities  $\vec{U}_{p_i}$  and  $\omega_{p_i}$ :

$$\begin{aligned} \rho \frac{D\vec{u}}{Dt} &= \nabla \cdot \boldsymbol{\sigma} + \vec{g} + \alpha \vec{l} - \mu \Delta \vec{l} && \text{in } \Omega \\ \nabla \cdot \vec{u} &= 0 && \text{in } \Omega \\ \int_{\Omega_{p_i}} (\rho_{p_i} - \rho_f) \frac{\partial \vec{U}_{p_i}}{\partial t} d\Omega_{p_i} &= \int_{\Omega_{p_i}} \rho_{p_i} \vec{g} - \nabla p - \alpha \vec{l} + \mu \Delta \vec{l} d\Omega_{p_i} + \vec{C}_{p_i} && \text{in } \Omega_{p_i} \\ \int_{\Omega_{p_i}} \omega_{p_i} d\Omega_{p_i} &= \frac{1}{2} \int_{\Omega_{p_i}} \nabla \times (\vec{u} - \vec{U}_{p_i}) d\Omega_{p_i} && \text{in } \Omega_{p_i} \end{aligned} \quad (5-4)$$

In addition to the system of equations 5-4, the rigid body constraint, the Lagrange multipliers and the particle advection equations must be included in the complete formulation:

$$\begin{aligned} \vec{l} &= 0 && \text{in } \Omega_f \\ \vec{u} &= \vec{U}_{p_i} + \omega_{p_i} \times (\vec{x} - \vec{X}_{p_i}) && \text{in } \Omega_{p_i} \\ \frac{\partial \vec{X}_{p_i}}{\partial t} &= \vec{U}_{p_i} && \text{for } p_i \in (1 \dots n_p) \end{aligned} \quad (5-5)$$

The variational formulation and the finite element discretization of the previous strong equations is exactly the same discussed in the previous chapter for flows with suspended particles. The only difference is the inclusion of the capillarity forces on the translational velocity equation of a particle  $p_i$  when it is over the two phase fluid interface.

We emphasize that previous works on floating particles that solves the Navier–Stokes equations only deals with particles that are initially at rest on the fluid interface. To the best of our knowledge this work is the first to simulate the full dynamics of the fluid–particle interaction, from the particle's flow inside the fluid phases until it reaches the equilibrium over the interface between two fluid phases.